# *Electronic Supplementary Information (ESI)*

## Organic derivatives of $Mg(BH_4)_2$ as precursors towards $MgB_2$ and novel inorganic mixed-cation borohydrides

W. Wegner,[a,b] T. Jaroń,[a]* M. A. Dobrowolski,[c] Ł. Dobrzycki,[c] M. K. Cyrański,[c] and W. Grochala[a]*

[a.] *Centre of New Technologies, University of Warsaw, Żwirki i Wigury 93, 02089 Warsaw, Poland. E-mail: tjaron@uw.edu.pl, w.grochala@cent.uw.edu.pl*
[b.] *College of Inter-Faculty Individual Studies in Mathematics and Natural Sciences, University of Warsaw, Stefana Banacha 2C, 02-097 Warsaw, Poland.*
[c.] *Advanced Crystal Engineering Laboratory (aceLAB), University of Warsaw, Żwirki i Wigury 101, 02089 Warsaw, Poland.*



## S1. Synthetic procedures

**$Mg(BH_4)_2$*1.5DME.**

40 ml of DME, 20 mmol (1.904 g) of $MgCl_2$ and 100 mmol (3.783 g) of $NaBH_4$ were introduced into a flat-bottomed flask and stirred for 7–22 h. After the reaction, NaCl and remaining $NaBH_4$ were separated by filtration using Schott filter, followed by rinsing the precipitation using 3x20 ml of DME. After evaporation of DME the residue was extracted using 60 ml of dichloromethane (DCM); typical yield: 75–85% (2.84–3.21 g).

**$Mg(BH_4)_2$*3THF.**

The mixture of 0.02 mol (1.904 g) of $MgCl_2$, 0.1 mol (3.783 g) of $NaBH_4$ and 40 ml of THF was stirred for 10 days in flat-bottomed flask with magnetic stirrer. After the synthesis, precipitate (PXD measurement showed unreacted $NaBH_4$ and unknown substance) was separated by filtration using Schott filter and washed using 50 ml of THF. Filtrate, containing the main product, was introduced to a rotary evaporator. Obtained residue was dissolved and filtered using 50 ml of DCM. The solvent was removed using rotary evaporator, which resulted in the final product.

**$[Me_4N]_2[Mg(BH_4)_4]$.**

There were 4 attempts to obtain this compound:

$MgCl_2 + 2LiBH_4 + 2Me4NBH_4 \rightarrow$ **$[Me4N]_2Mg(BH_4)_4$** + 2LiCl (S1)
$Mg(BH_4)_2 + 2Me4NBH_4 \rightarrow$ **$[Me4N]_2Mg(BH_4)_4$**(S2)
$Mg(BH_4)_2 + Me4NBH_4 \rightarrow$ **$[Me4N]Mg(BH_4)_3$** (S3)
$Mg(BH_4)_2$*1.5DME+ $2Me4NBH_4 \rightarrow$ **$[Me4N]_2Mg(BH_4)_4$** +1.5DME (S4)

The first three were the mechanochemical reactions, where the reagents were milled for 30 min. The fourth one was a solvent-mediated reaction. In this case 2 mmol (378 mg) of $Mg(BH_4)_2$*1.5DME with 4 mmol (356 mg) of TMAB ($Me_4NBH_4$) were mixed in 30 ml of DCM for 16 h in flat-bottomed flask with magnetic stirrer. After the reaction, the main product was filtered and washed with 20 ml of DCM. The residue (main product) was freed from solvent by vacuum evaporation. The filtrate was investigated after removing solvent in evaporator – only unreacted $Mg(BH_4)_2$*1.5DME was found there.

**Procedure for synthesis of $[n\text{-}(C_4H_9)_4N]_xMg(BH_4)_4$.**

Three following attempts were tested:

$$MgCl_2 + 2LiBH_4 + 2(n\text{-}C_4H_9)_4NBH_4 \rightarrow [(n\text{-}C_4H_9)_4N]_2Mg(BH_4)_4 + 2LiCl \quad (S5)$$

$$Mg(BH_4)_2 + (n\text{-}C_4H_9)_4NBH_4 \rightarrow [(n\text{-}C_4H_9)_4N]Mg(BH_4)_3 + 2LiCl \quad (S6)$$

$$Mg(BH_4)_2{*}1.5DME + 2(n\text{-}C_4H_9)_4NBH_4 \rightarrow [(n\text{-}C_4H_9)_4N]_2Mg(BH_4)_4 + 1.5DME \quad (S7)$$

The first two were the mechanochemical reactions, where reagents were milled for 30 min, in 5 min cycles. The third one was a solvent-mediated reaction between 2 mmol (378 mg) of $Mg(BH_4)_2{*}1.5DME$ and 4 mmol (1029 mg) of TBAB ($(n\text{-}C_4H_9)_4NBH_4$). They were dissolved in 30ml of DCM and mixed together for 24.5 h in flat-bottomed flask equipped in a magnetic stirrer. After the reaction mixture was transferred to a round bottom flask with addition of 5 ml of DCM. The next step was solvent removal using evaporator, which resulted in obtaining oil-like substance. The final step was an overnight drying *in vacuo*.

**$[(C_6H_5)_4P]_2Mg(BH_4)_4$.**

The mixture of 7.5 mmol (1.419 g) of $Mg(BH_4)_2{*}1.5DME$ with 15 mmol (5.314 g) of $(C_6H_5)_4PBH_4$ was stirred in 100 ml of DCM for 24 h in a flat-bottomed flask equipped with a magnetic stirrer. After the synthesis the sample was freed from solvent using a rotary evaporator. Next step was to dissolve it, filter it and wash it using 160 ml of diethyl ether. After removing of the solvent, the final product was collected from the filter. Reaction yield of at 98.9% (7.541 g) was significantly higher than in literature (74.6%), probably due to much longer (12-fold) reaction time.

**$Li_xMg(BH_4)_{2+x}$.**

There were two attempts to obtain lithium magnesium borohydride, assuming:

$$2LiBH_4 + Mg(BH_4)_2 \rightarrow \mathbf{Li_2Mg(BH_4)_4} \quad (S8)$$

$$[(C_6H_5)_4P]_2Mg(BH_4)_4 + 2Li[Al(OC(CF_3)_3)_4] \rightarrow \mathbf{Li_2Mg(BH_4)_4}\downarrow + 2[(C_6H_5)_4P][Al(OC(CF_3)_3)_4] \quad (S9)$$

Reaction (S8) was a mechanochemical reaction. Substrates, 6mmol of $LiBH_4$(131 mg) and 3mmol(162 mg) of γ-$Mg(BH_4)_2$,were milled for 40 min. In solvent-mediated reaction (S9) 0.55 mmol (419 mg) of $[(C_6H_5)_4P]_2Mg(BH_4)_4$ was dissolved in 10 ml of $CH_2Cl_2$and 1 mmol (974 mg) of $Li[Al(OC(CF_3)_3)_4]$ was dissolved in 50 ml of $CH_2Cl_2$.Both solutions and needed equipment were cooled down to -35 °C before the synthesis. After that, both solutions were mixed together and stirred for 30 min in RT. After the reaction, formed precipitate was filtered and placed in -35 °C. Resulting deposit was heavier (87 mg) then expected (56 mg).

**$Na_xMg(BH_4)_{2+x}$.**

The reaction attempts proceeded according to the following routes:

$$[(C_6H_5)_4P]_2Mg(BH_4)_4 + 2Na[BAr^F_4] \rightarrow \mathbf{Na_2Mg(BH_4)_4}\downarrow + 2[(C_6H_5)_4P][BAr^F_4] \quad (S10)$$

$$[(C_6H_5)_4P]_2Mg(BH_4)_4 + 3Na[Al(OC(CF_3)_3)_4] \rightarrow \mathbf{Na_2Mg(BH_4)_4}\downarrow + 2[(C_6H_5)_4P][Al(OC(CF_3)_3)_4] + Na[Al(OC(CF_3)_3)_4] \quad (S11)$$

where $[BAr^F_4]$= $[B[3,5\text{-}(CF_3)_2C_6H_3]_4]$.In reaction (S10) 1mM of $Na[BAr^F_4]$ was mixed with 0.55 mmol of $[(C_6H_5)_4P]_2Mg(BH_4)_4$in 50 ml of DCM for 1 h, in RT. In reaction (S11) 0.55 mmol (419 mg) of $[(C_6H_5)_4P]_2Mg(BH_4)_4$dissolved in 10 ml of DCM was mixed with 1.5 mmol of $Na[Al(OC(CF_3)_3)_4]$ (1485 mg, ~50% excess) dissolved in 90 ml of DCM. Before this reaction solutions and needed equipment were cooled down to -35 °C. After that, both solutions were stirred after mixing for 30 min in RT. Formed precipitate was filtered, placed in vacuum for 5 min and then placed in -35 °C.

**$K_xMg(BH_4)_{2+x}$.**

There were two attempts to obtain potassium magnesium borohydride, assuming:

$$[(C_6H_5)_4P]_2Mg(BH_4)_4 + 2K[Al(OC(CF_3)_3)_4] \rightarrow \mathbf{K_2Mg(BH_4)_4}\downarrow + 2[(C_6H_5)_4P][Al(OC(CF_3)_3)_4] \quad (S12)$$

$$[(C_6H_5)_4P]_2Mg(BH_4)_4 + K[Al(OC(CF_3)_3)_4] \rightarrow \mathbf{K_2Mg(BH_4)_4}\downarrow + [(C_6H_5)_4P][Al(OC(CF_3)_3)_4] + 0.5[(C_6H_5)_4P]_2Mg(BH_4)_4 \quad (S13)$$

In reaction (S12) 0.55 mmol (419 mg) of $[(C_6H_5)_4P]_2Mg(BH_4)_4$ was dissolved in 10 ml of DCM and mixed with 1 mmol (1.006g) of $K[Al(OC(CF_3)_3)_4]$ dissolved in 10 ml of DCM. After that, both solutions were stirred for ~2h

in RT. Formed precipitate was filtered and placed in vacuum. Mass of precipitate was 77 mg (in the case of formation only $K_2Mg(BH_4)_4$, reaction yield would be 95.1%).

In reaction (S13) 0.22 mmol (excess, 168 mg) of $[(C_6H_5)_4P]_2Mg(BH_4)_4$ was dissolved in 10 ml of DCM and mixed with 0.22 mmol (220 mg) of $K[Al(OC(CF_3)_3)_4]$ dissolved in 20 ml of DCM. After that, both solutions were stirred for 50 min in RT. Formed precipitate was filtered and placed in vacuum. Mass of precipitate was 24 mg.

**$Rb_3Mg(BH_4)_5$.**

The reaction was assumed to proceed according to the following route:

$$[(C_6H_5)_4P]_2Mg(BH_4)_4 + 2Rb[Al(OC(CF_3)_3)_4] \rightarrow \mathbf{Rb_2Mg(BH_4)_4}\downarrow + 2[(C_6H_5)_4P][Al(OC(CF_3)_3)_4] \quad (S14)$$

In reaction (S14) 0.55 mmol (419 mg) of $[(C_6H_5)_4P]_2Mg(BH_4)_4$ was mixed with 1 mmol (1053 mg) of $Rb[Al(OC(CF_3)_3)_4]$ in 50 ml of DCM ($CH_2Cl_2$). The mixture was stirred for 19 h, and then filtered and washed with 10 ml of DCM.

**Procedure for synthesis of $Cs_3Mg(BH_4)_5$.**

The reactions proceeds according to the following assumed schedules:

$$Mg(BH_4)_2 + 2CsBH_4 \rightarrow \mathbf{Cs_2Mg(BH_4)_4} \quad (S15)$$

$$MgCl_2 + 2LiBH_4 + 3CsBH_4 \rightarrow \mathbf{Cs_3Mg(BH_4)_5} + LiCl \quad (S16)$$

$$[(C_6H_5)_4P]_2Mg(BH_4)_4 + 2Cs[Al(OC(CF_3)_3)_4] \rightarrow \mathbf{Cs_2Mg(BH_4)_4}\downarrow + 2[(C_6H_5)_4P][Al(OC(CF_3)_3)_4] \quad (S17)$$

In reactions (S15) and (S16) substrates were mixed in *ca.* 1:2, 1:2:3 molar ratio (162 : 887 mg, 191 : 88 : 887 mg), respectively. In both reactions, reagents were milled for 40 min in an Ar atmosphere in a stainless steel disc bowl. Reaction (S17) was carried out in 0.55 : 1 mmol stoichiometry (419 : 1100 mg). In this case, each substrate was dissolved in 25 ml of DCM. Both solutions were next mixed together, and stirred for 22 h in RT. After that, main product was filtered and washed with 25 ml of DCM.

## S2. Li-Mg systems

The freshly-prepared lithium-containing precipitate, besides $LiBH_4$, LiCl and $Li[Al(pftb)_4]$, reveals also the absorption bands characteristic for $[Ph_4P]_2[Mg(BH_4)_4]$ and a set of diffraction peaks from a novel phase(s). After *ca.* 2 d the signals of $Li[Al(pftb)_4]$ completely vanish from the diffraction pattern (Fig. S9), which occurs simultaneously with the drop of intensity of the absorption band at *ca.* 1094 $cm^{-1}$ and the intensity increase of the band 1122 $cm^{-1}$, both characteristic to the $\delta_{H-B-H}$ vibrations of various borohydrides, Fig. S8. It seems that the reaction is ongoing slowly between the precursors occluded in the products. The set of PXD peaks from the novel phase can be indexed in an orthorhombic unit cell belonging to $Pna2_1$ extinction class, a = 17.534 Å, b = 19.365 Å, c = 14.563 Å, V = 4945.0 $Å^3$ (*cf.* Fig. S14 - LeBail fit), however, due to the quality of diffraction pattern and large unit cell, the structure solution and full identification of this phase have been unsuccessful. It is worth to mention here that $Li^+$ cations show tendency to form $LiMg(BH_4)_4^-$ layers in trimetallic borohydrides containing magnesium, promoting rather complicated topologies which might result in larger unit cells of related compounds.[i]

## S3. Rb-Mg and Cs-Mg systems

Ad. (3): Besides $Mg(BH_4)_2$, rather weak absorption bands originating from the organic precursors are visible in FTIR spectra. However the reaction yield exceeds the expected on the basis of reaction stoichiometry (up to *ca.* 120%), which indicates rather significant contamination. This has been further discussed together with the time-resolved MS results of the gaseous products evolved during thermal decomposition of $M_3Mg(BH_4)_5$ compounds.

## S4. XPS analysis

$Mg(BH_4)_2 \cdot 1.5DME$ heated up to 450 °C and commercially available $MgB_2$ have been analyzed also using X-ray photoelectron spectroscopy (XPS), Fig. S26. Both samples show deficiency of the lighter B, however, the determined Mg : B ratio is closer to stoichiometric for the decomposed solvate, Tab. S1. Rather high and comparable amount of oxygen is found in both samples which mostly reflects the surface contamination by this ubiquitous element of strong affinity to Mg, as XPS reveals sensitivity restricted to several dozens of atomic layers. Indeed, the oxygen contamination is detected by XPS in $MgB_2$ carefully prepared via different synthetic methods

even in the oxygen-limited environment.[ii],[iii] Interestingly, although the organic impurities containing C–H bonds were detected by the means of FTIR spectroscopy in the product of thermal decomposition of $Mg(BH_4)_2$·1.5DME contrary to the commercially available $MgB_2$, the latter shows significantly higher level of surface contamination with adventitious carbon. The minor extraneous elements might either be the impurities of the precursors of $MgB_2$ (like Ca in case of commercial $MgB_2$), or were introduced during the synthetic procedure (like Si probably from the glass frit applied for preparation of $Mg(BH_4)_2$·1.5DME).

Table S1. Elemental analysis according to XPS for commercial $MgB_2$, $Mg(BH_4)_2$·1.5DME heated up to 450 °C.

| XPS peak | Commercial $MgB_2$ [at%]# | $Mg(BH_4)_2$·1.5DME heated to 450 °C [at%]* |
|---|---|---|
| **Mg 2s** | **17.3** | **18.2** |
| **B 1s** | **15.4** | **27.2** |
| C 1s | 22.0 | 14.7 |
| O 1s | 36.1 | 37.2 |
| Ca 2p | 6.3 | - |

# also <1.8 at% F, Fe, Cr detected; * also <2.3 at% Si, F, Na detected

## S5. PXRD patterns, FTIR & XPS & MS spectra and structures addons

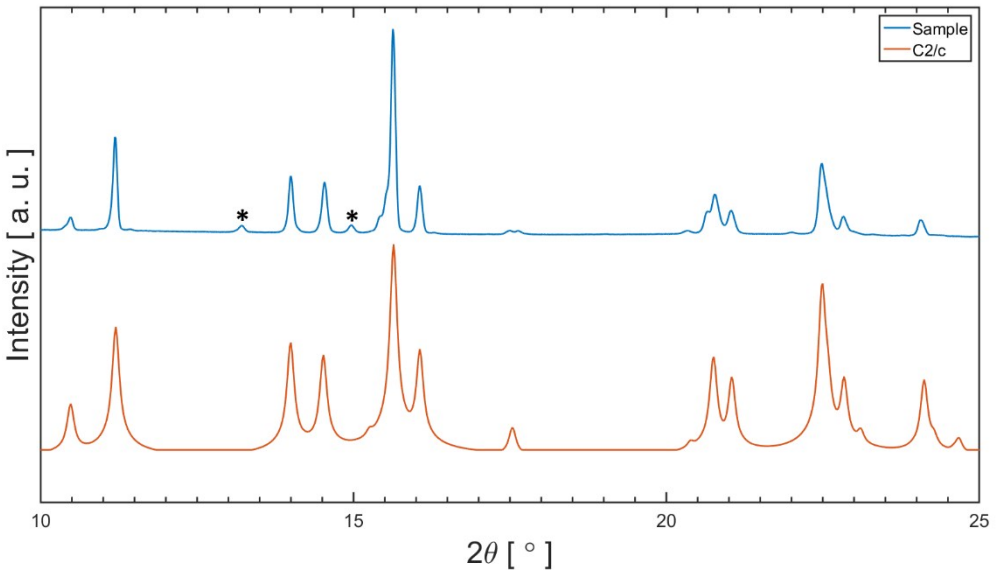


*Figure S1. Comparison of PXD measurements for synthesized $Mg(BH_4)_2$*3THF sample (top) with its simulated, known C2/c structure (bottom). * – unknown phase.*[iv]

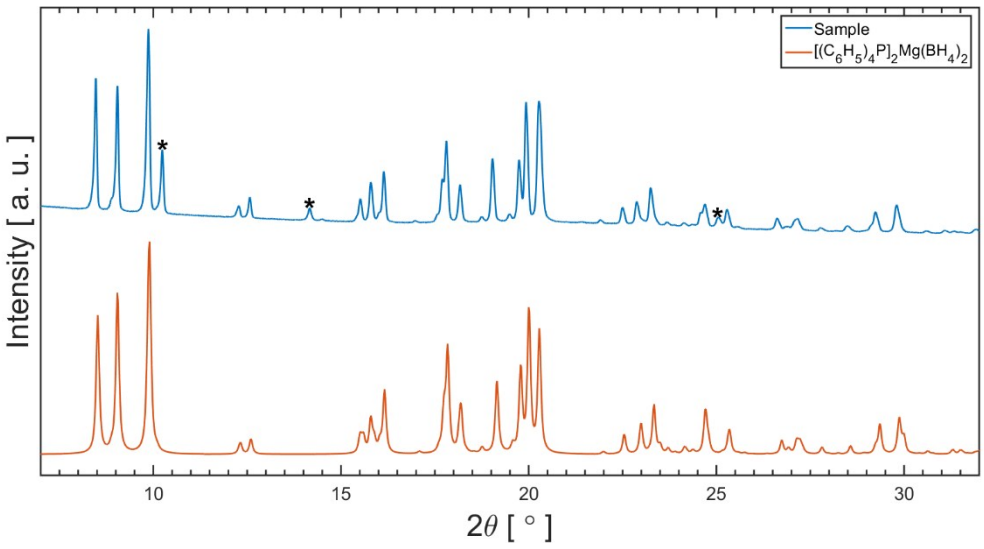


*Figure S2. Comparison of sample PXD measurement after $[(C_6H_5)_4P]_2Mg(BH_4)_4$ synthesis (top) with the pattern simulated as based on the published structure (bottom).*[v]

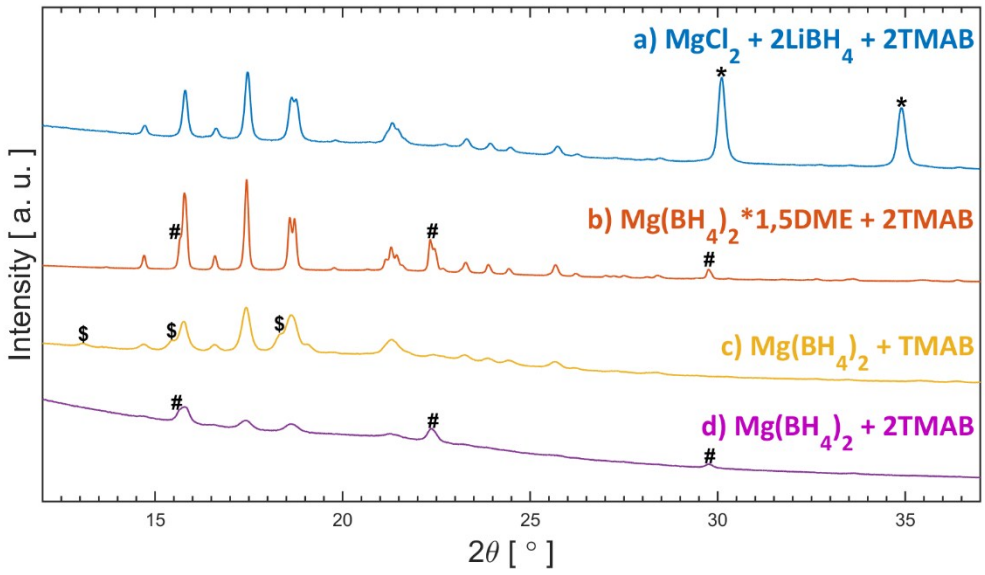


*Figure S3. Comparison of PXRD measurements for different synthetic routes of $[(CH_3)_4N]_2Mg(BH_4)_4$. *-LiCl, #-TMAB, $-unknown phase, $[(CH_3)_4N]_2Mg(BH_4)_4$ – unmarked reflections.*

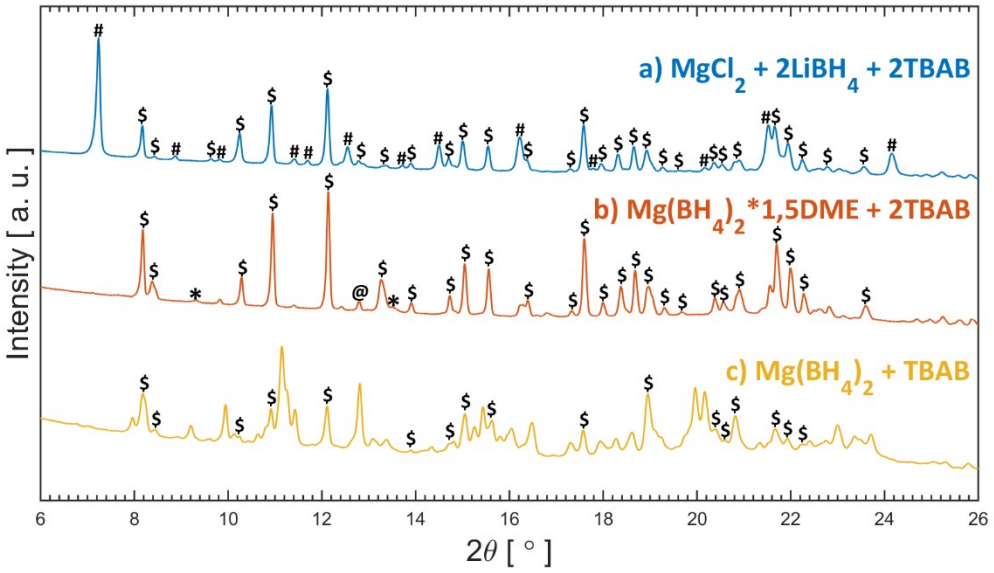


*Figure S4. Comparison of PXD measurements for different synthetic routes for $[(n\text{-}C_4H_9)_4N]_2Mg(BH_4)_4$. *-TBAB, $- phase with unchanged intensity after ~8 months, #- phase with change intensity after~8 months, @-$Mg(BH_4)_2$*1.5DME.*

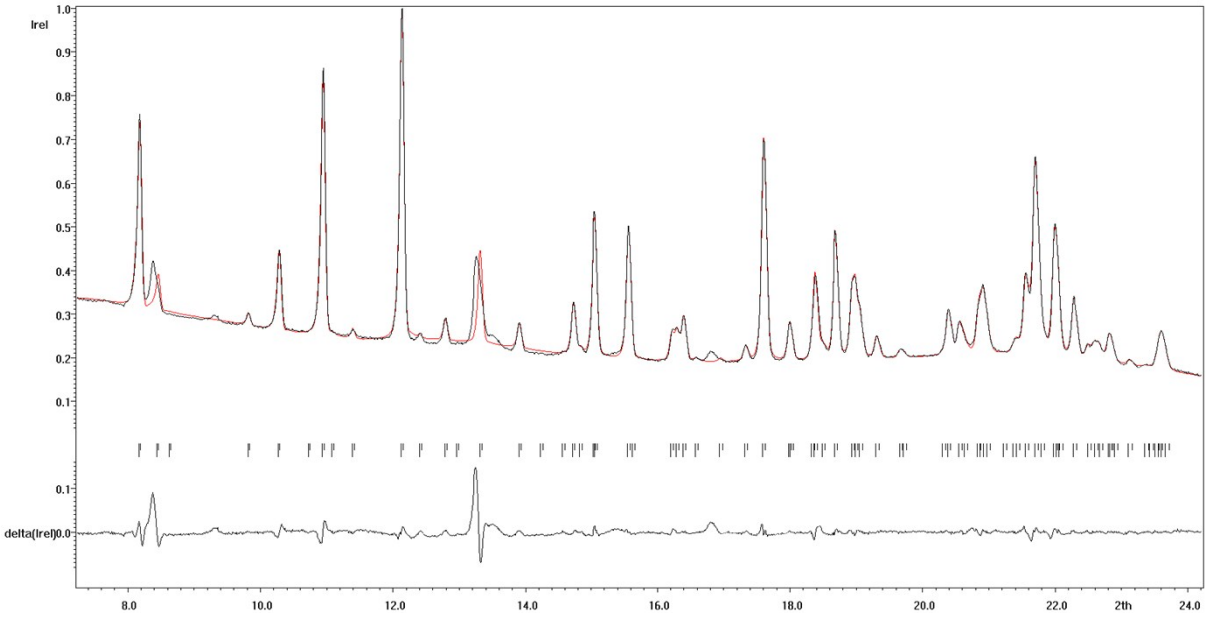


*Figure S5. The Le-Bail refinement for the products of reaction between $Mg(BH_4)_2 \cdot 1.5DME$ and $[nBu_4N]BH_4$ in DCM. The tetragonal unit cell: $I4_1/a$), a = 25.459(10) Å, c = 34.407(14) Å, V = 22302(18) Å$^3$ has been refined. Due to complexity of the powder pattern, only the low-angle part has been presented.*

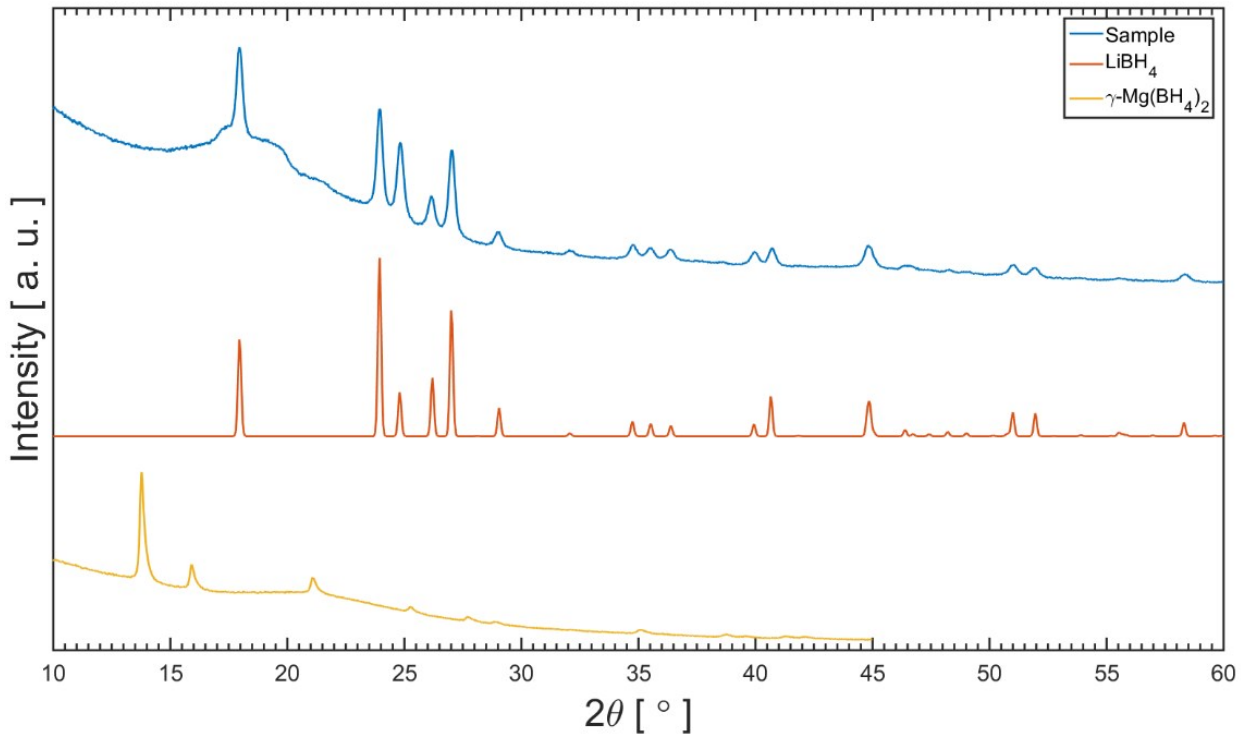


*Figure S6. Comparison of PXRD measurements for product of the reaction no. S8 (attempt to synthesize $Li_xMg(BH_4)_{2+x}$) with the diffraction patterns of the reagents.*

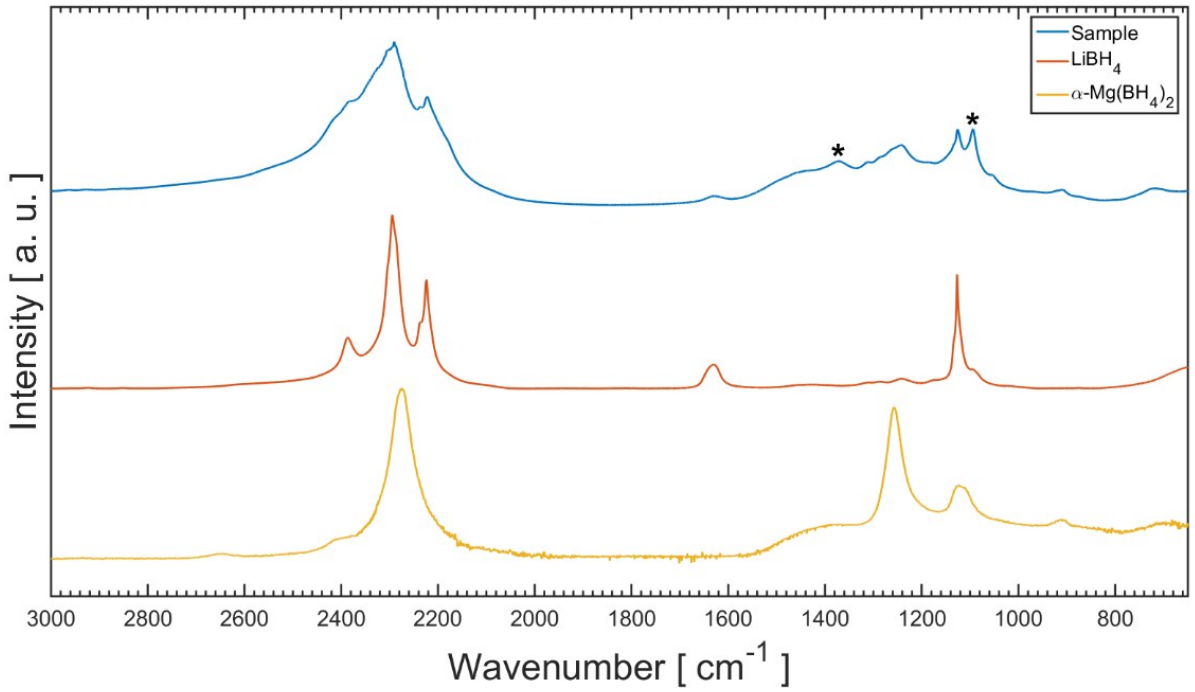


*Figure S7. Comparison of FTIR spectra for: product of the reaction no. S8 (attempt to synthesize $Li_xMg(BH_4)_{2+x}$) and of the substrates.*[v]

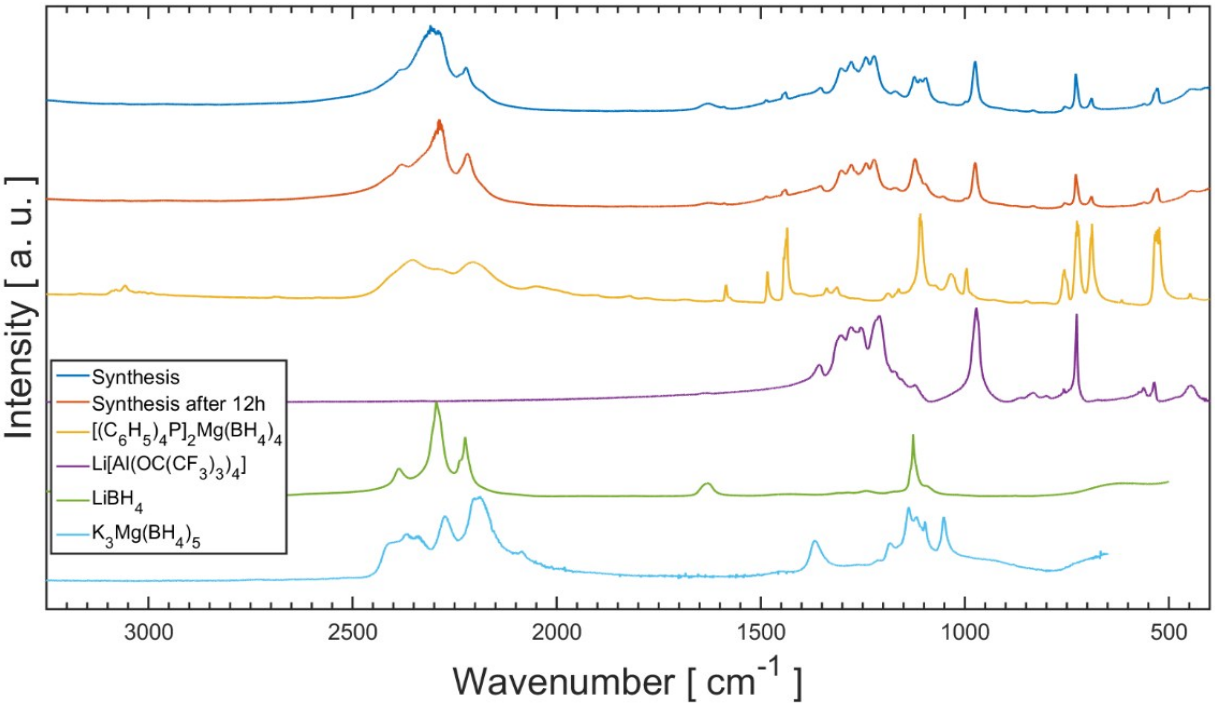


*Figure S8. Comparison of FTIR spectrum for product of reaction no. S9 (attempt to synthesize $Li_xMg(BH_4)_{2+x}$) with spectra of the substrates and of the possible products.*

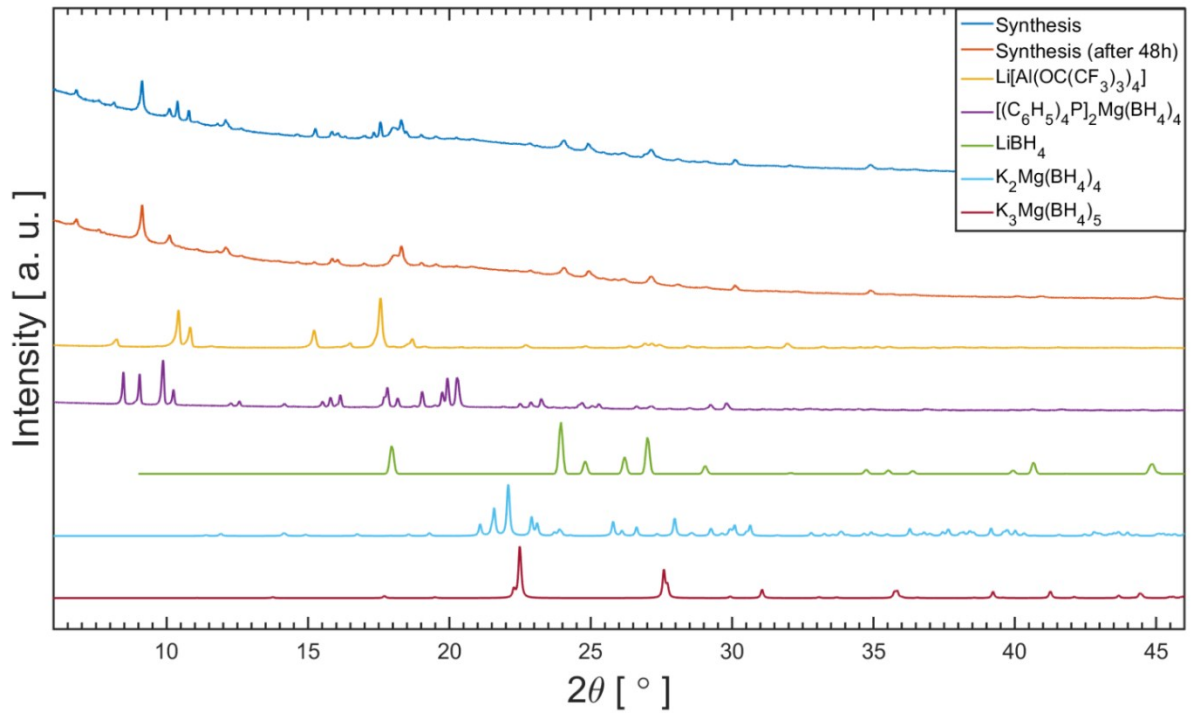


*Figure S9. Comparison of PXRD pattern for product of reaction no. S9 (attempt to synthesize $Li_xMg(BH_4)_{2+x}$) with diffraction patterns from the substrates and possible products.*[vi]

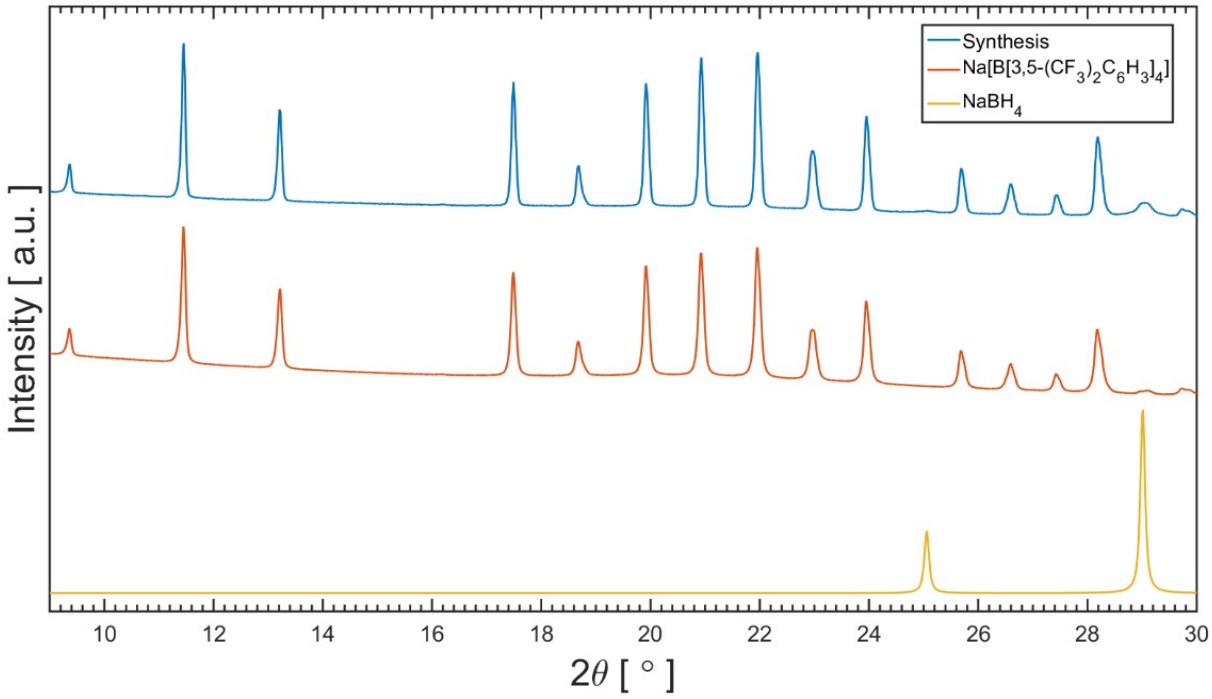


*Figure S10. PXRD measurement of sample after reaction no. S10 (attempt to synthesized $Na_xMg(BH_4)_{2+x}$) with XRD patterns from the substrate and $NaBH_4$.*

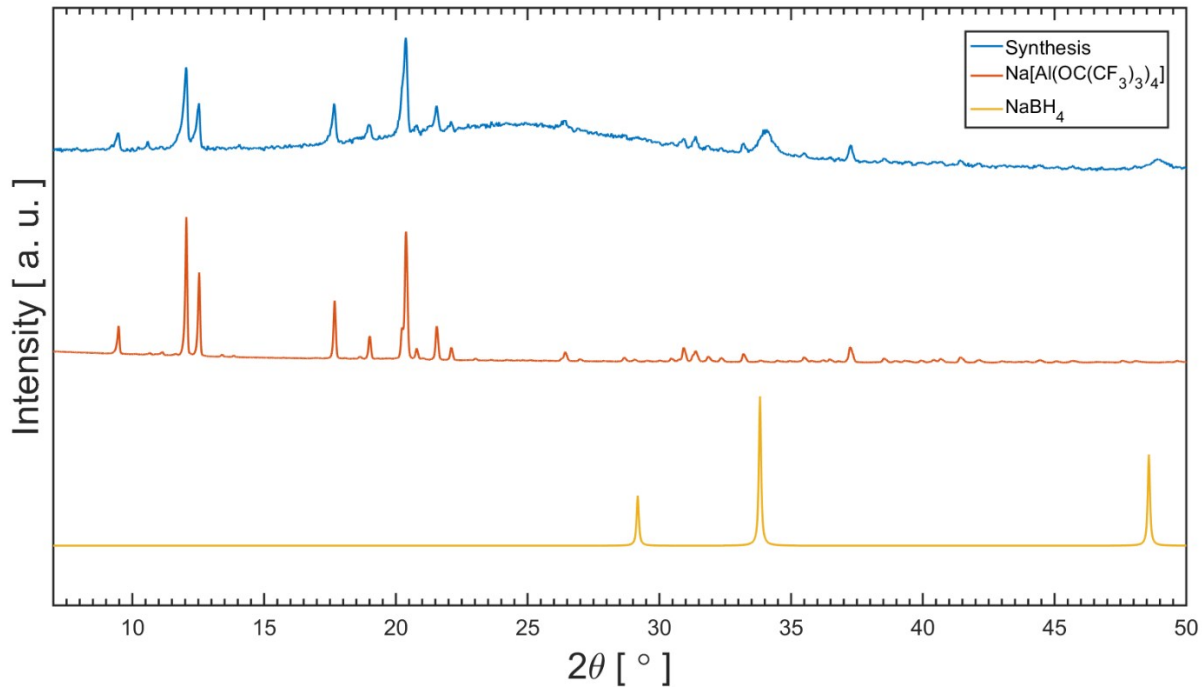


*Figure S11. PXRD measurement of sample after reaction no. S11 (attempt to synthesized $Na_xMg(BH_4)_{2+x}$) with XRD patterns from the substrate and $NaBH_4$.*

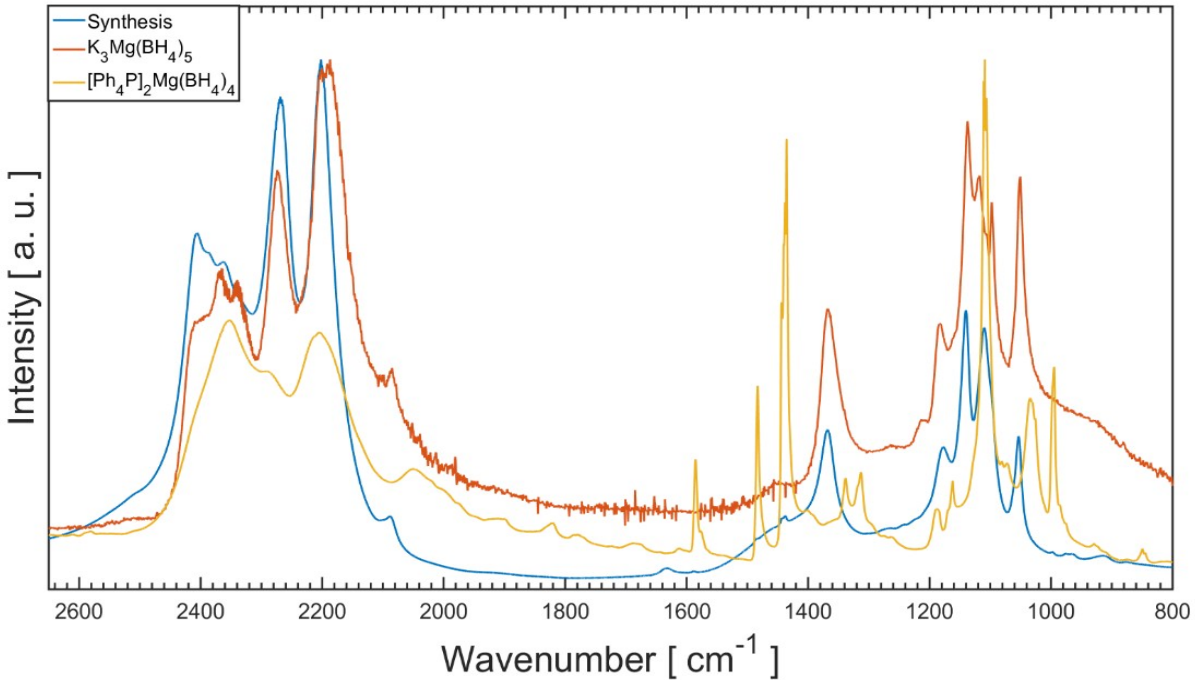


*Figure S12. Comparison of FTIR spectra of: $M_3Mg(BH_4)_5$, M =$K^{vii}$, Rb and $[(C_6H_5)_4P]_2Mg(BH_4)_4$.*

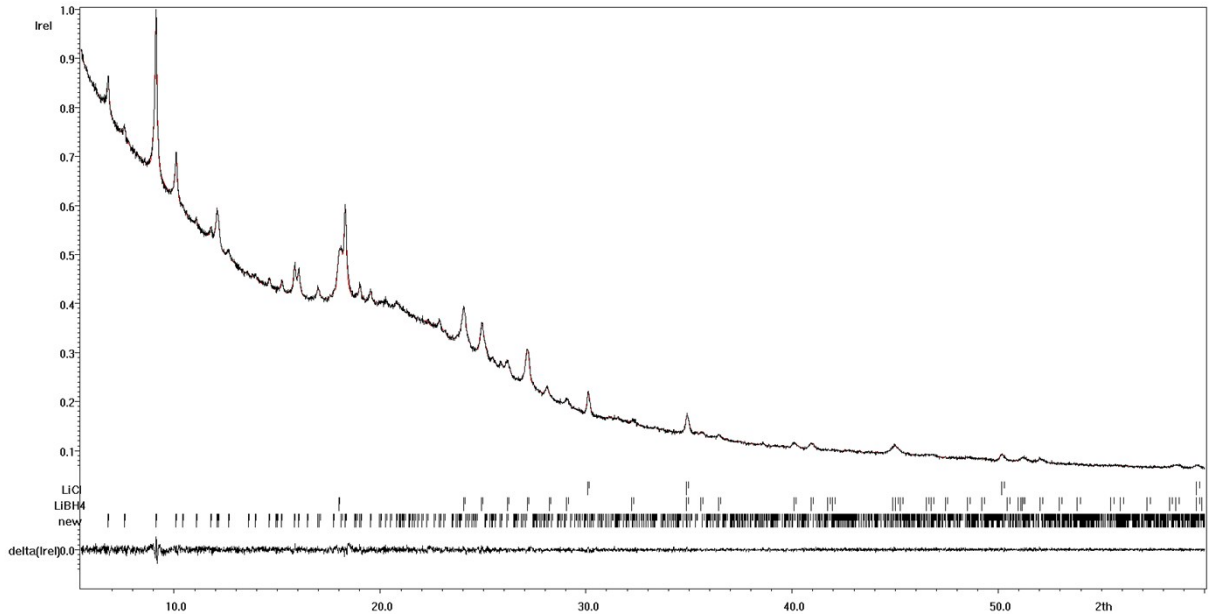


*Figure S13. The Le-Bail refinement for the products of reaction between $Li[Al(pftb)_4]$ and $[Ph_4P]_2[Mg(BH_4)_4]$ after ca. 2 d at room temperature. The orthorhombic unit cell used for fitting: $Pna2_1$, a = 17.534 Å, b = 19.365 Å, c = 14.563 Å, V = 4945.0 $Å^3$.*

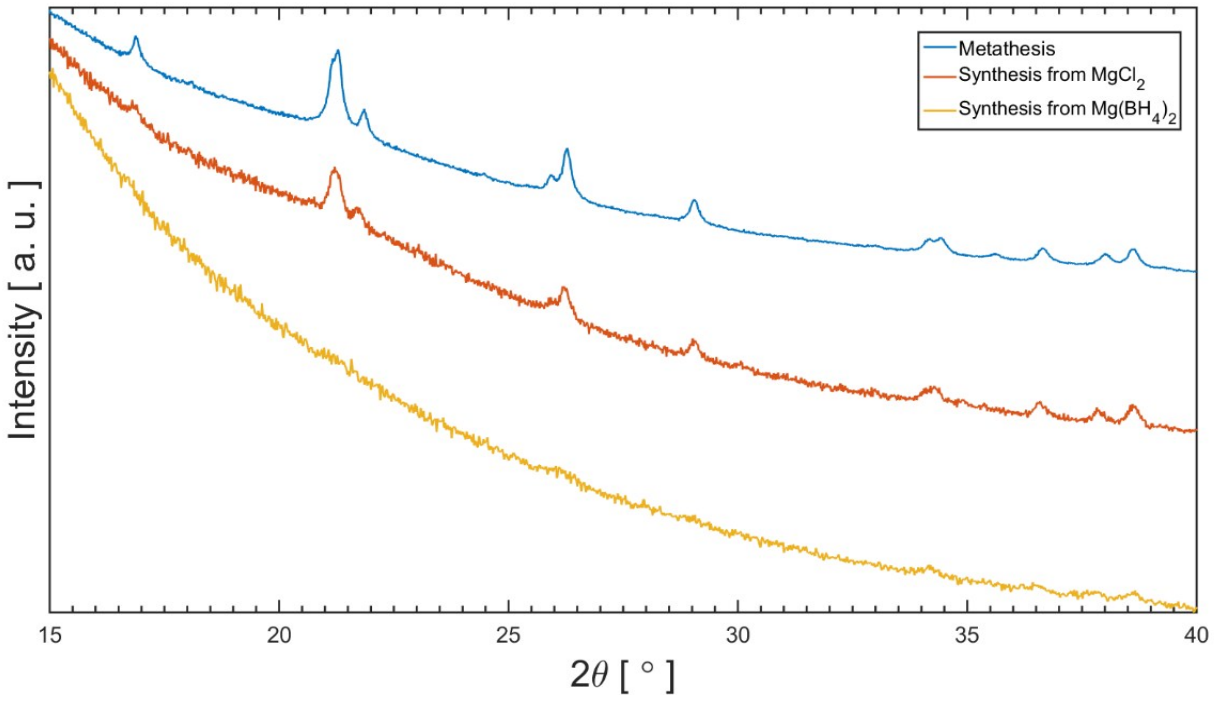


*Figure S14. Comparison of PXRD measurements for 3 different synthetic routes for $Cs_xMg(BH_4)_{2+x}$: solvent-mediated metathesis, eqs. (1), (3); mechanochemical synthesis from $MgCl_2$, eq. (4); mechanochemical synthesis from $Mg(BH_4)_2$, eq. (5).*

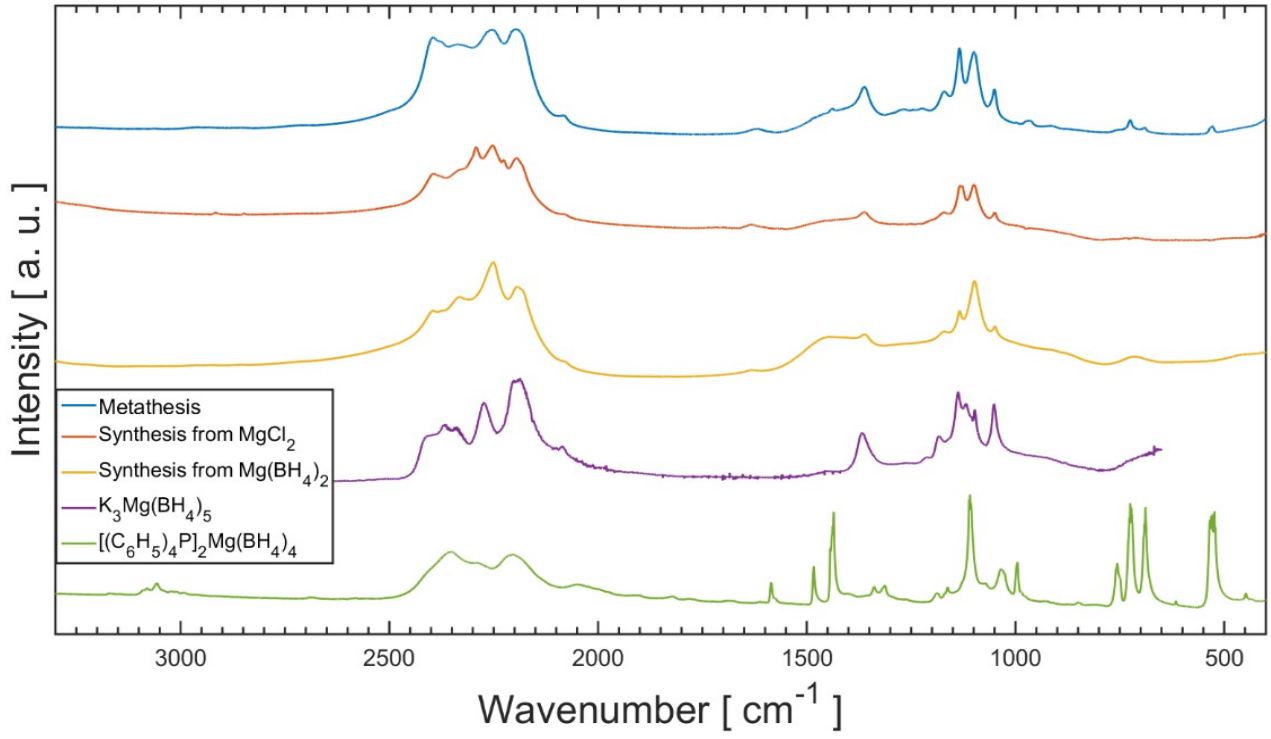


*Figure S15. Comparison of FTIR spectra for 3 different synthetic routes for $Cs_xMg(BH_4)_{2+x}$ and spectra of the substrates and possible products.*[v]

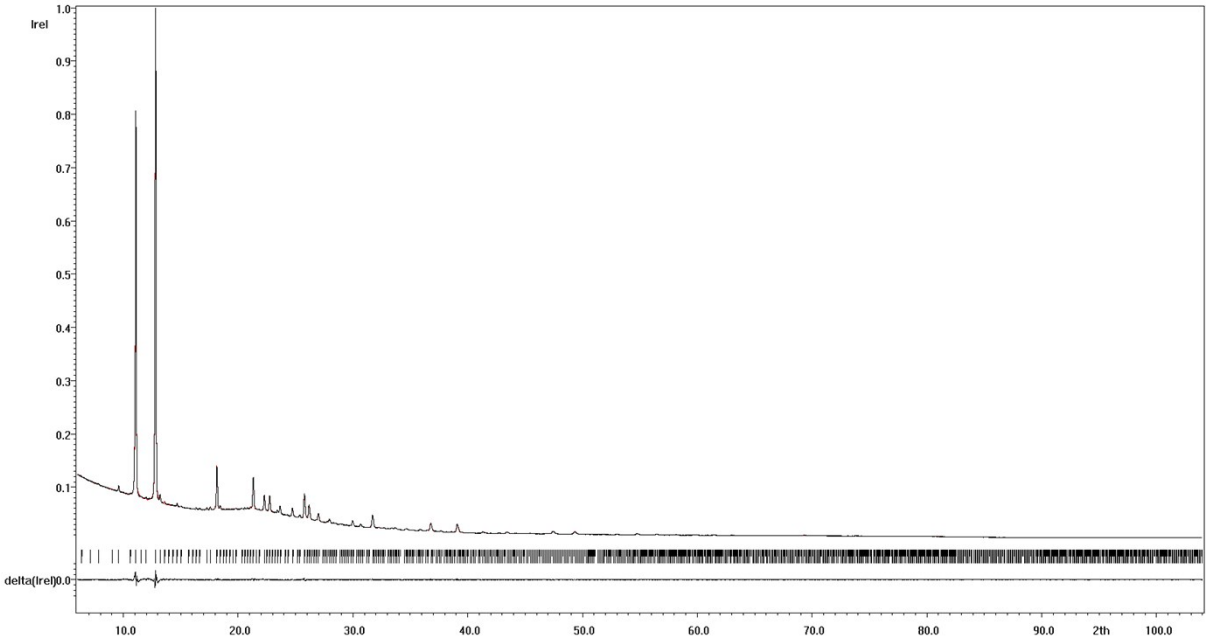


*Figure S16. The Le-Bail refinement of the PXD measured for $Mg(BH_4)_2$·1.5DME ( room temperature).*

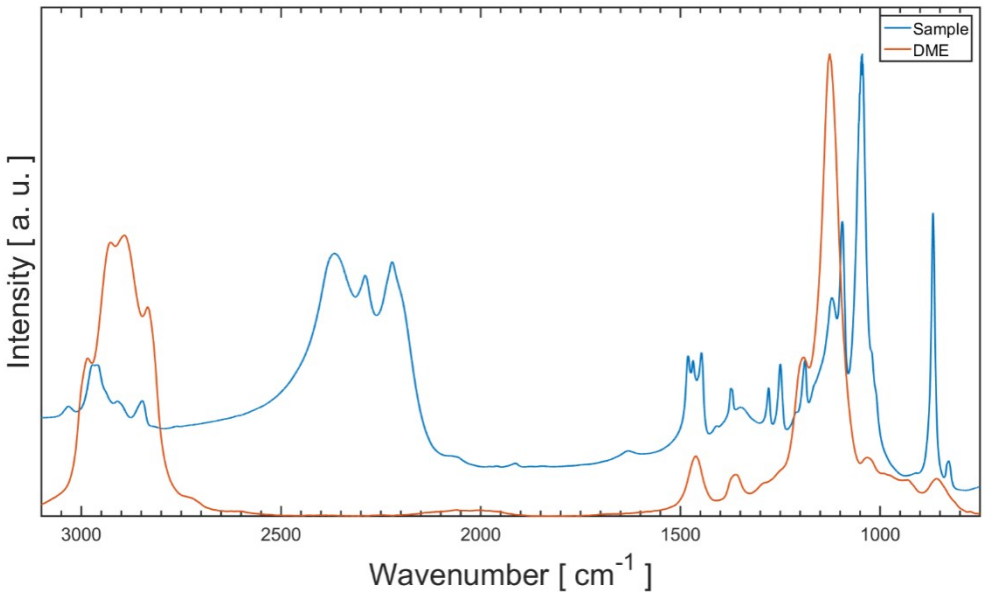


*Figure S17. Comparison of FTIR spectra of $Mg(BH_4)_2$*1.5DME and liquid DME.*[viii]

Table S2. Crystal data and structure refinement for $Mg(BH_4)_2 \cdot 1.5DME$.

| **Identification code** | **$Mg(BH_4)_2 \cdot 1.5DME$** |
|---|---|
| **Chemical formula** | $C_{96}H_{353}B_{32}Mg_{16}O_{48}$ |
| ***M*** | 3011.64 |
| ***T*/ K** | 100(2) |
| ***λ*/ Å** | 1.54178 |
| **Crystal size** | 0.160×0.208×0.278 |
| **Unit cell dimensions** | *a*=27.2332(9) |
| **Volume** | 20197.(2) |
| ***Z*** | 4 |
| ***$D_x$*/ g cm$^{-3}$** | 0.990 |
| ***μ*/ mm$^{-1}$** | 1.001 |
| ***F*(000)** | 6660 |
| ***$\theta_{min}$* ,*$\theta_{max}$*** | 2.29 to 58.95° |
| **Index ranges** | -24≤h≤29, -18≤k≤30, -26≤l≤30 |
| **Reflections collected** | 49819 |
| **Independent reflections** | 5027 [R(int) = 0.0510] |
| ***$T_{max}$*, *$T_{min}$*** | 0.7516 and 0.6228 |
| **Refinement method** | Full-matrix LSQ on $F^2$ |
| **Data / restraints / parameters** | 5027 / 150 / 542 |
| **GooF** | 1.038 |
| **Final *R* indices** | 4220 data; $I>2\sigma(I)$<br>$R1$ = 0.0652, $wR2$ = 0.1931<br>all data<br>$R1$ = 0.0791, $wR2$ = 0.2162 |
| ***$\rho_{max}$*, *$\rho_{min}$*/ eÅ$^{-3}$** | 0.291 and -0.362 eÅ$^{-3}$ |

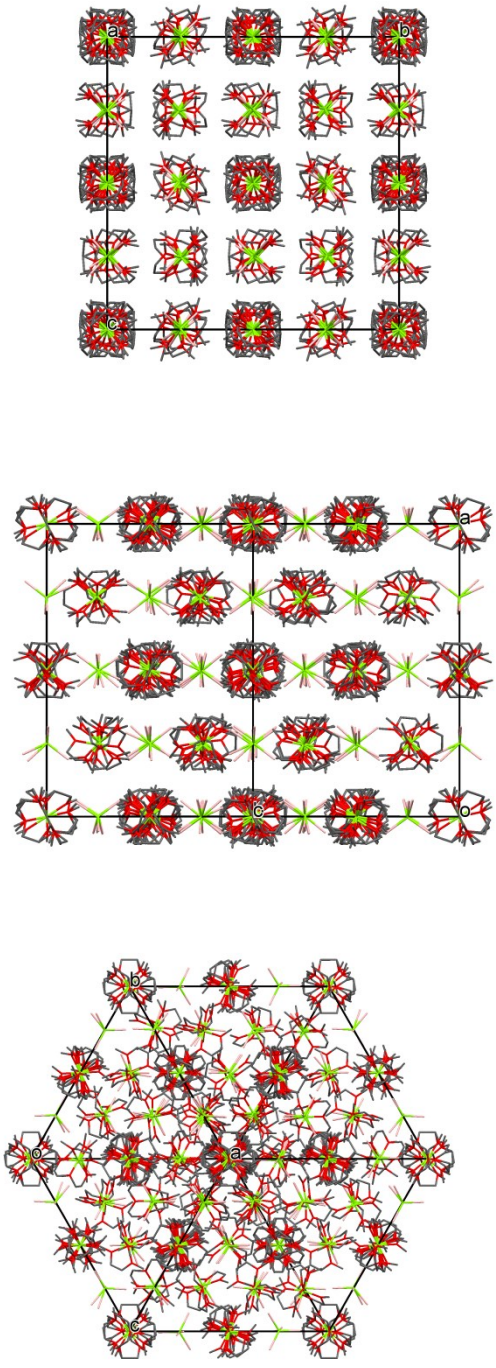


*Figure S18. Structure of $Mg(BH_4)_2$*1.5DME. Packing along: top –100; middle – 110; bottom – 111.*

Table S3. Unit cells parameters for obtained and refined $M_3Mg(BH_4)_5$ phases, M = Rb, Cs and $K_3Mg(BH_4)_5$.

| | $K_3Mg(BH_4)_5$[vi] | **$Rb_3Mg(BH_4)_5$** | **$Cs_3Mg(BH_4)_5$** |
|---|---|---|---|
| **Space group** | *P* $4_2$/m b c | *I* 4/m c m | *I* 4/m c m |
| **a** [Å] | 8.9693(6) | 9.2996(14) | 9.7115(4) |
| **b** [Å] | 8.9693(6) | 9.2996(14) | 9.7115(4) |
| **c** [Å] | 15.9501(13) | 15.993(2) | 16.2540(8) |
| **V** [Å$^3$] | 1283.15(19) | 1383.1(4) | 1532.97(15) |

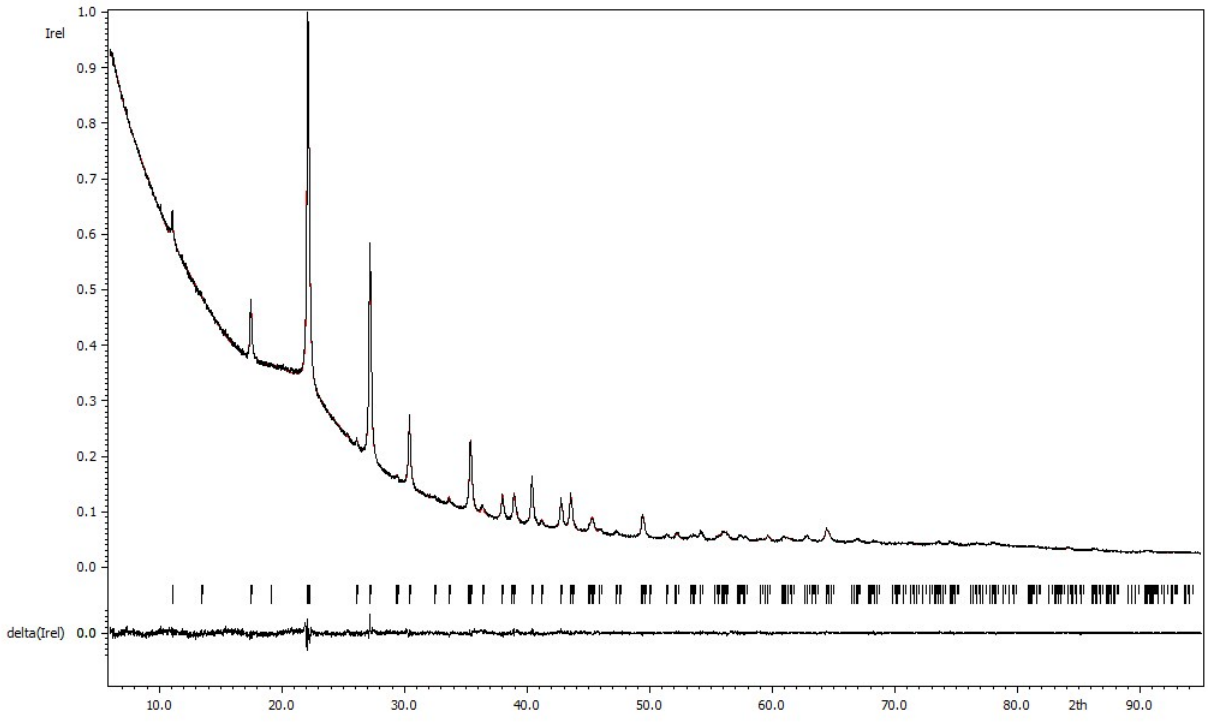


*Figure S19. Rietveld refinement of $Rb_3Mg(BH_4)_5$. Black – experimental data, red – calculated curve. Below are the position of the reflections and the difference between the experimental and calculated profile.*

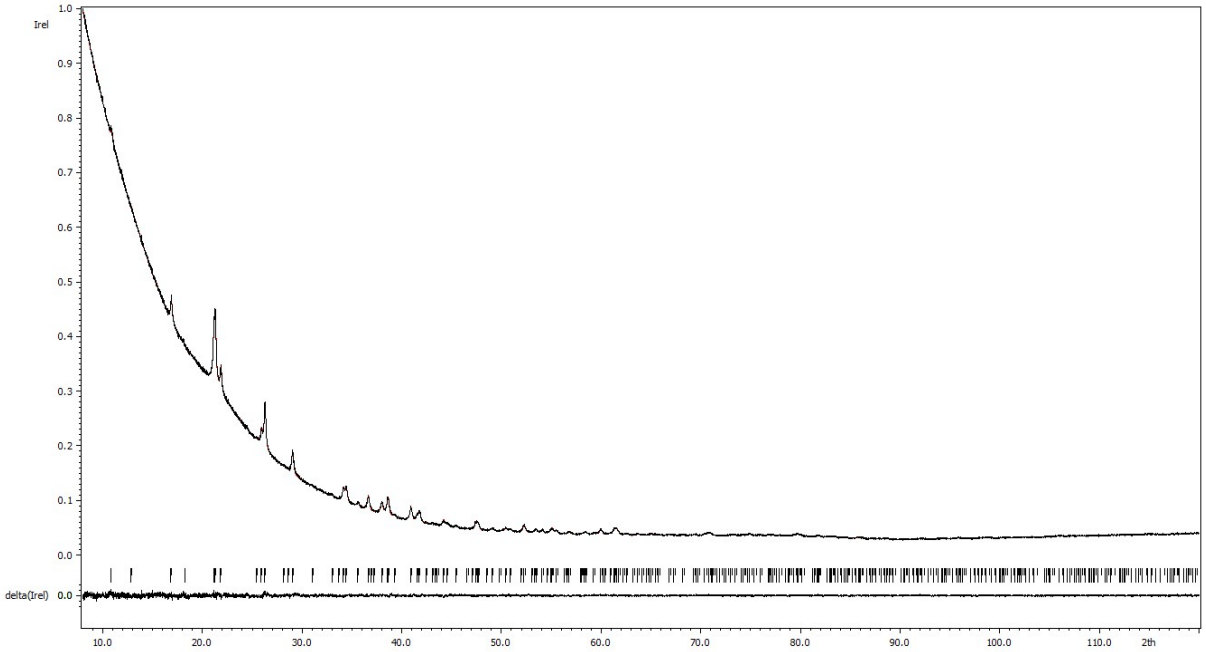


*Figure S20. Rietveld refinement of $Cs_3Mg(BH_4)_5$. Black – experimental data, red – calculated curve. Below are the position of the reflections and the difference between the experimental and calculated profile.*

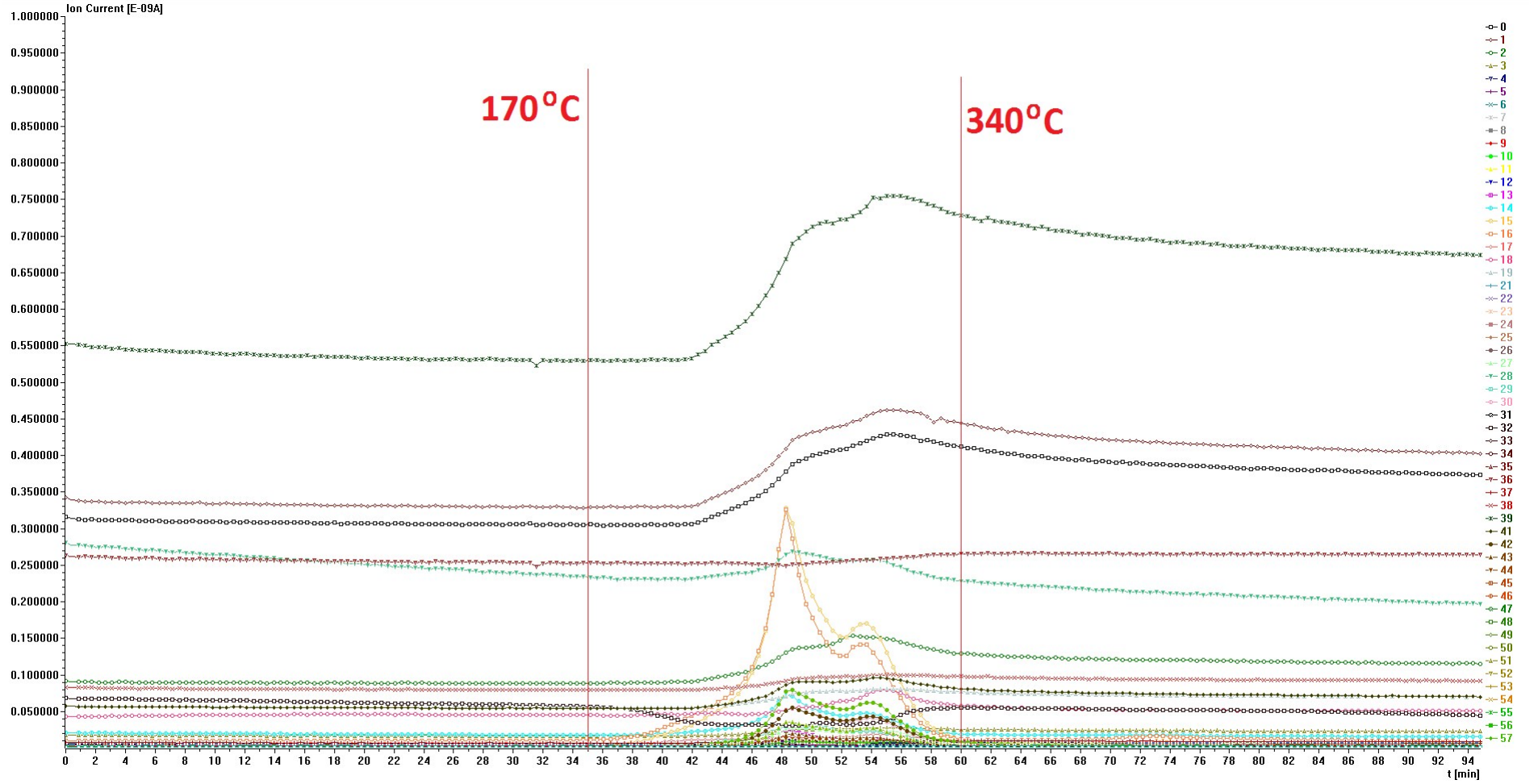


*Figure S21. Time-resolved MS spectra of the gaseous products of thermal decomposition of $[Me_4N]_2[Mg(BH_4)_4]$; heating rate: 5 °C $min^{-1}$.*

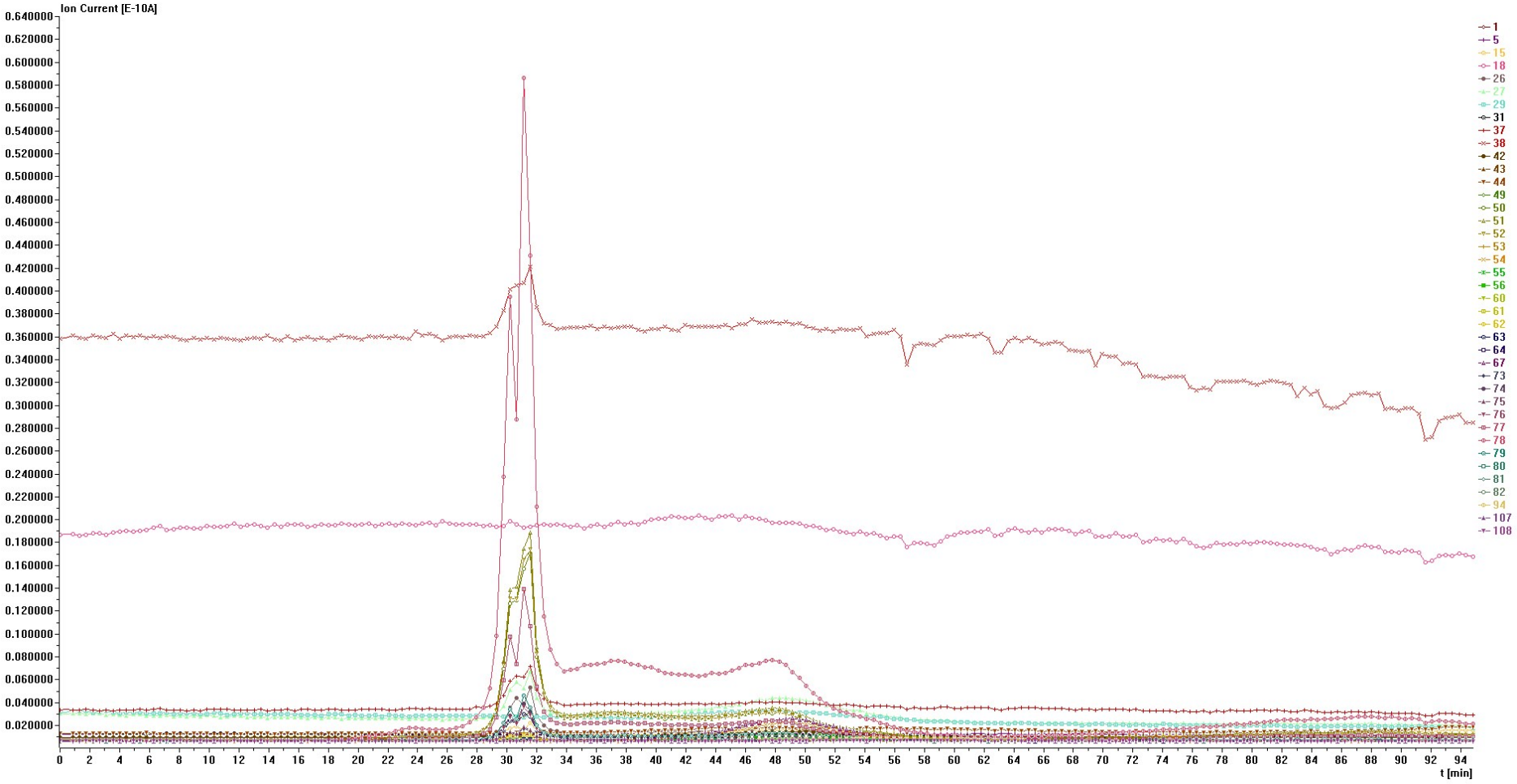


*Figure S22. Time-resolved MS spectra of the gaseous products of thermal decomposition of $[Ph_4P]_2[Mg(BH_4)_4]$; heating rate: 5 $^oC\ min^{-1}$.*

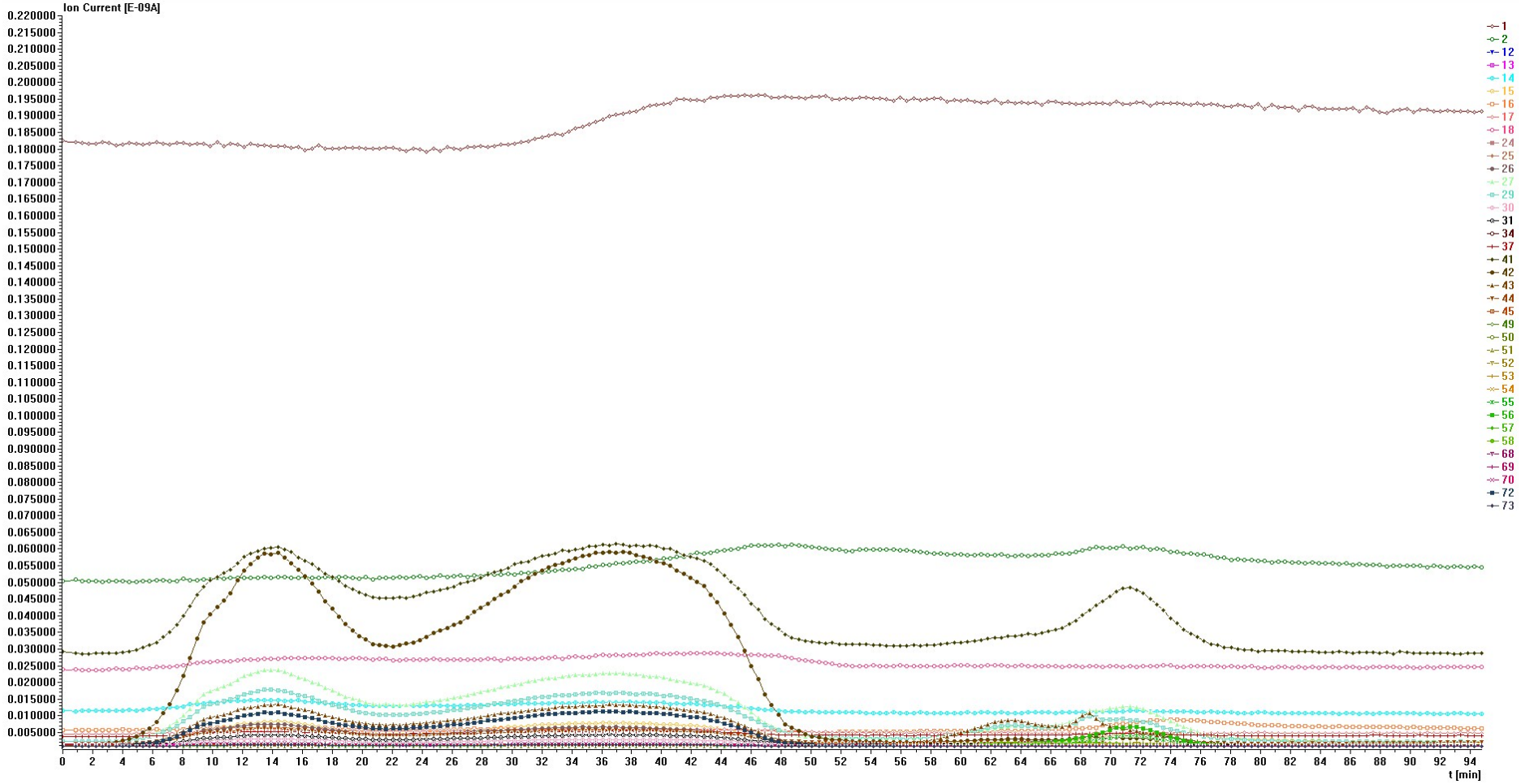


*Figure S23. Time-resolved MS spectra of the gaseous products of thermal decomposition of $Mg(BH_4)_2 \cdot 3THF$; heating rate: 5 °C $min^{-1}$.*

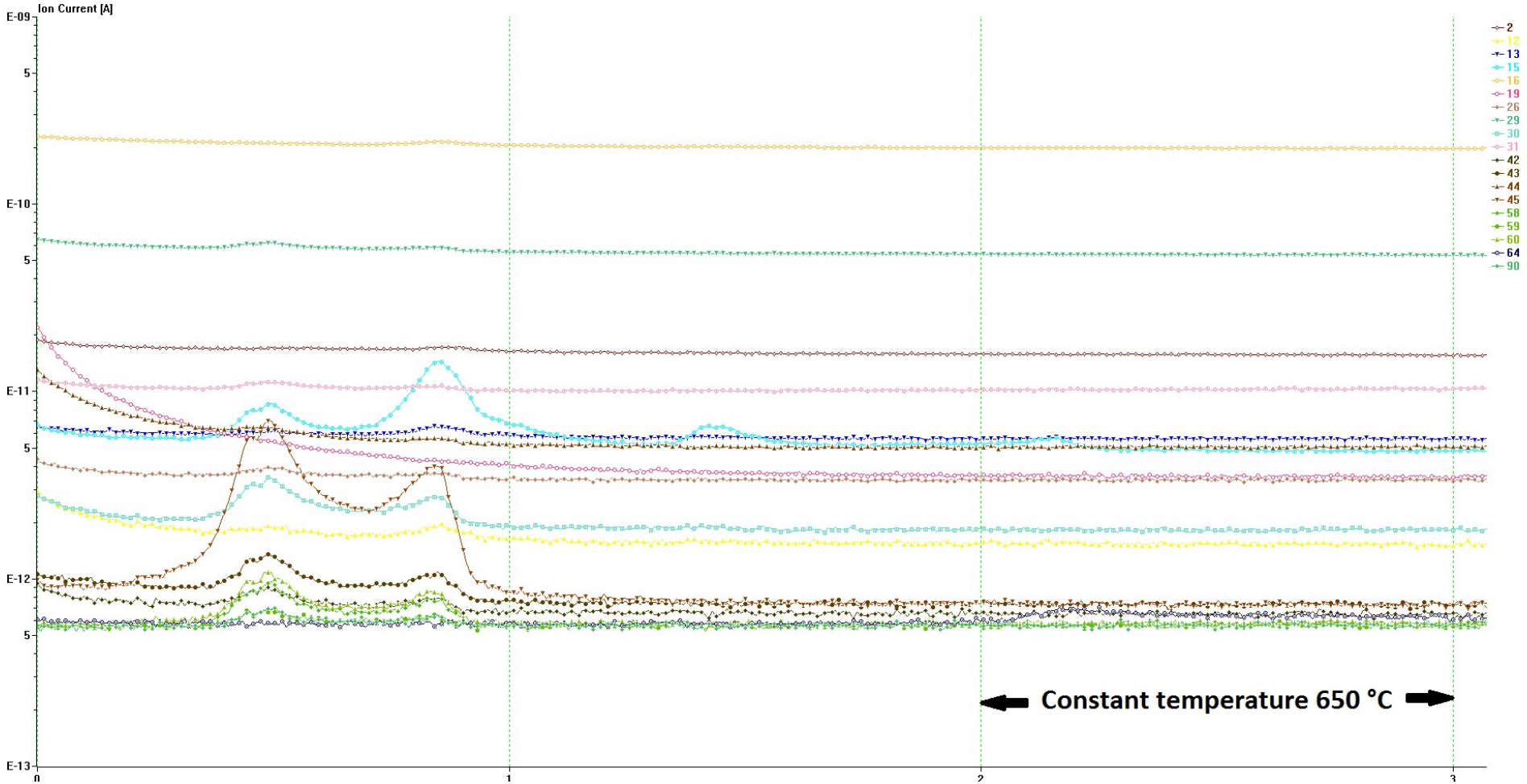


*Figure S24. Time-resolved MS spectra of the gaseous products of thermal decomposition of $Mg(BH_4)_2 \cdot 1.5DME$; heating rate: 5 °C $min^{-1}$ followed by isothermal scan at 650 °C.*

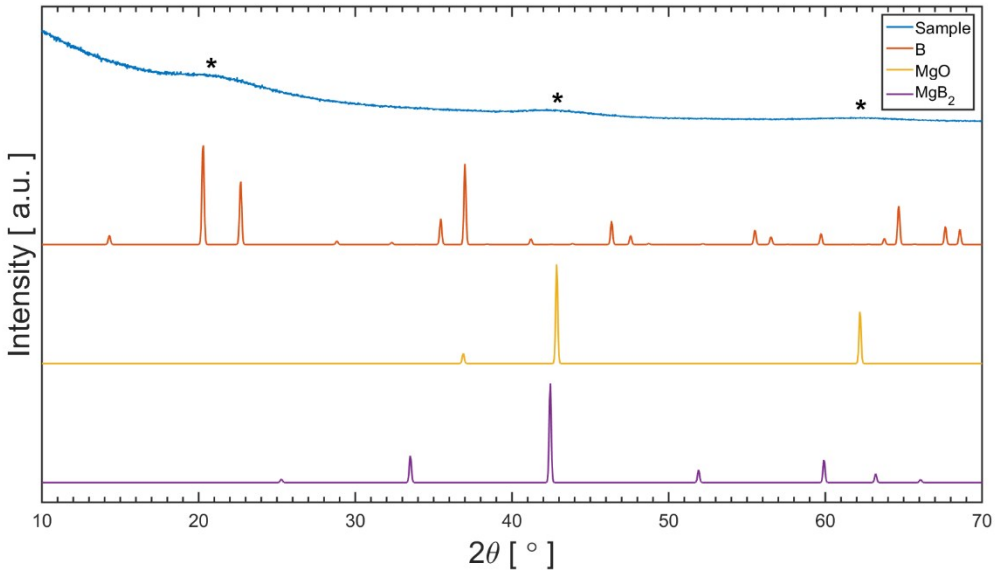


*Figure S25. Comparison of PXRD measurement of $Mg(BH_4)_2$*3THF heated to 500 °C with simulated diffraction patterns for B, MgO and $MgB_2$. * - weak, broad signals.*

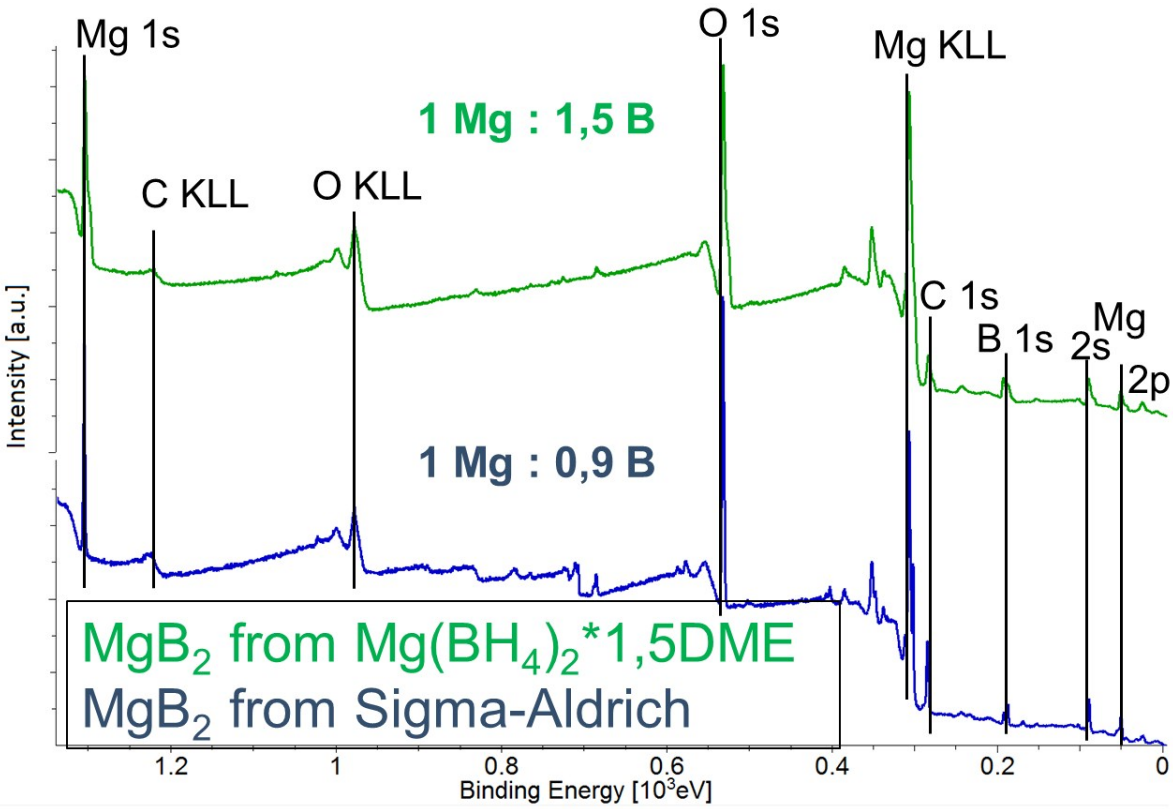


*Figure S26. The survey XPS spectra of $Mg(BH_4)_2$*1.5DME heated to 450 °C and commercial $MgB_2$. The electron flood gun for charging compensation has been applied. The electron current of 5 µA and the electron energy of 1V were applied for commercially available $MgB_2$, while 20 µA and 8 V were used for the measurements of the decomposed sample of $Mg(BH_4)_2$*1.5DME.*

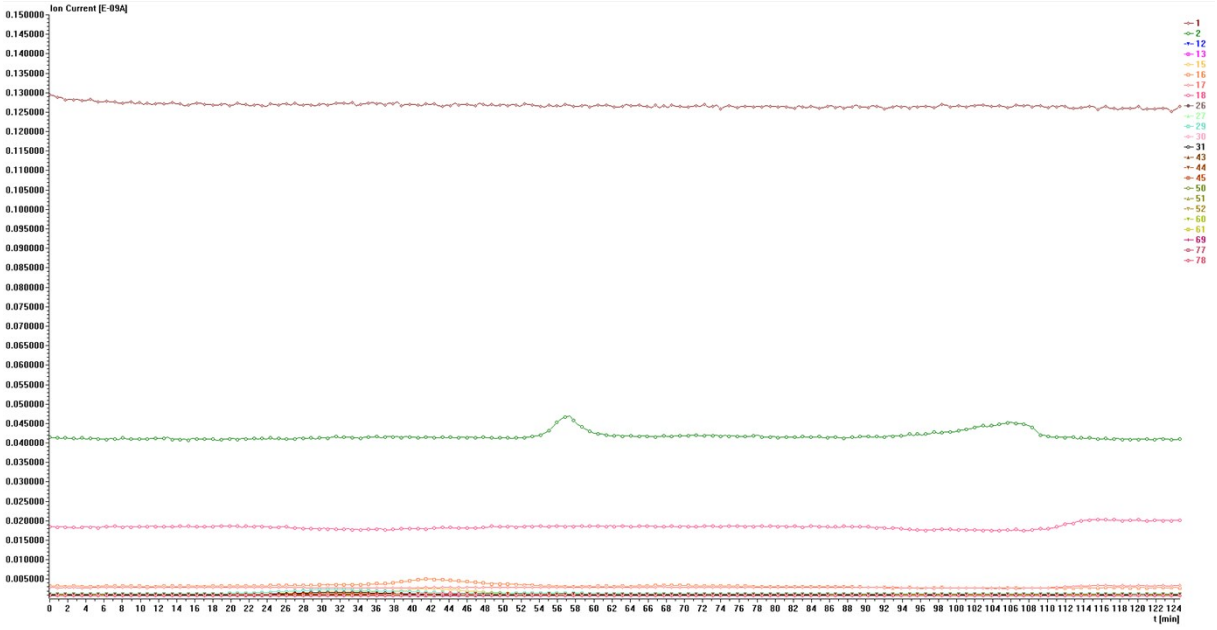


*Figure S27. Time-resolved MS spectra of the gaseous products of thermal decomposition of $Rb_3Mg(BH_4)_5$ prepared using a solvent-mediated method of synthesis; heating rate: 5 $^oC\ min^{-1}$.*

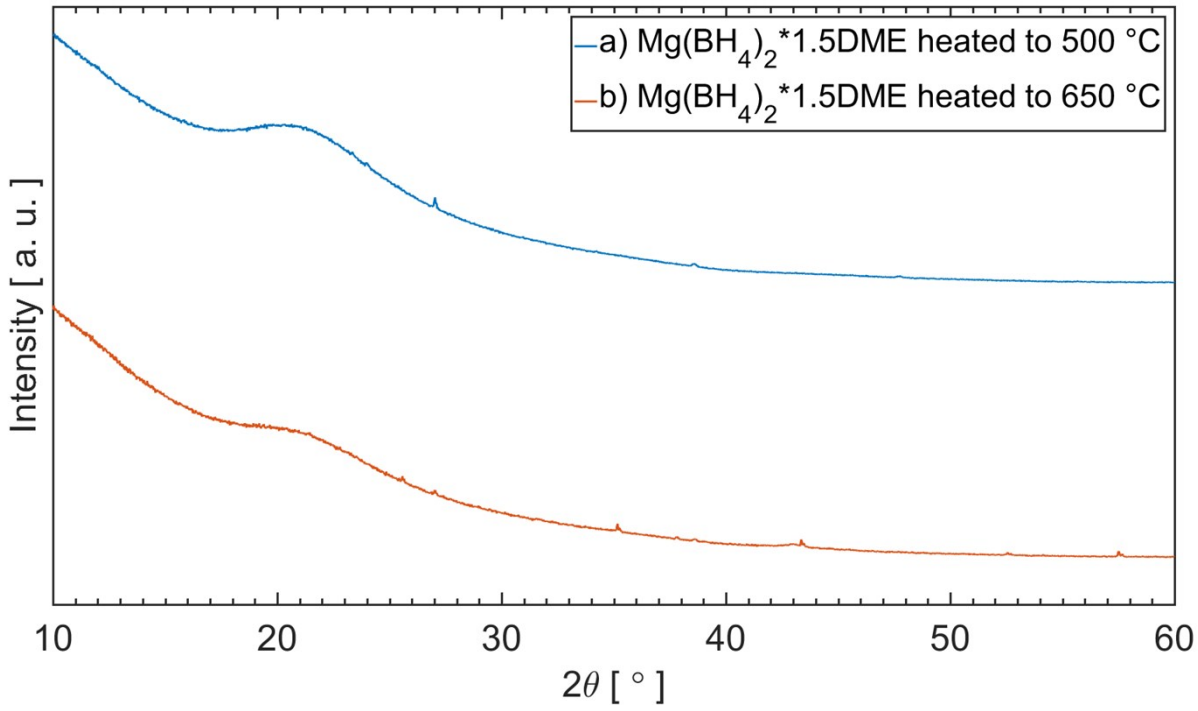


*Figure S28. PXRD measurement of $Mg(BH_4)_2$*1.5DME heated to a) 500 °C, b)650 °C. In a) weak reflection from unknown substance emerge, same as in b), where also $Al_2O_3$ reflection can be seen (crucible material).*

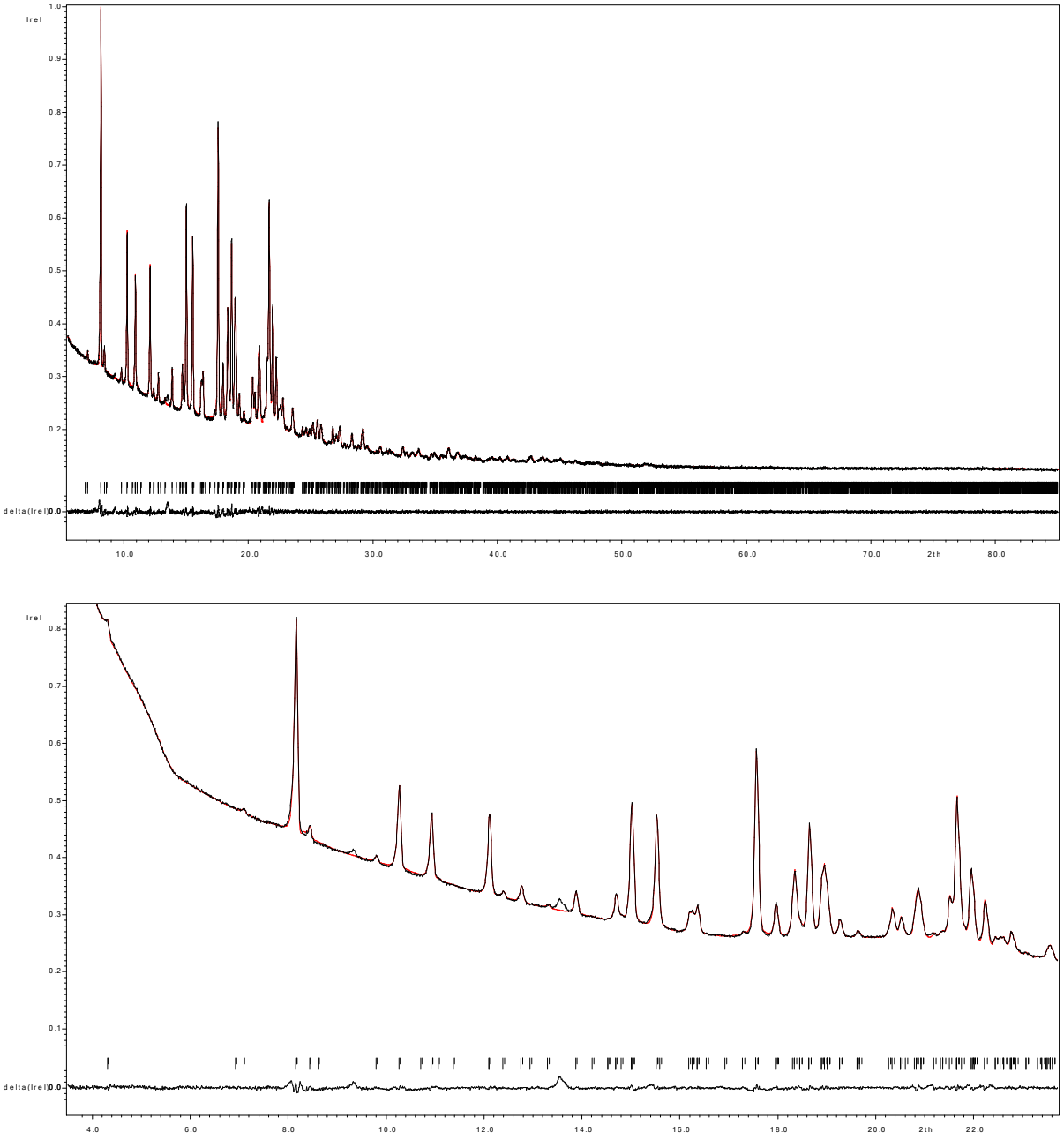


*Figure S29. The Le-Bail refinement for $[n\text{-}(C_4H_9)_4N]_2Mn(BH_4)_4$. Black – experimental data, red – calculated curve. Below are the position of the reflections and the difference between the experimental and calculated profile.*

## S6. Thermal decomposition of $M_3Mg(BH_4)_5$, M=Rb, Cs

As it has been discussed, the $M_3Mg(BH_4)_5$ compounds prepared using a solvent-mediated method of synthesis contain *ca.* 33 mol% of amorphous $Mg(BH_4)_2$, eq. (3), while also the occluded organic precursors might be also present. On the other side, the mechanochemical method of preparation results in the products contaminated with LiCl or unreacted precursors, as it has been exemplified by $Cs_3Mg(BH_4)_5$, eqs. (4) and (5). Thermal decomposition process is clearly influenced by these additives, Fig. S30.

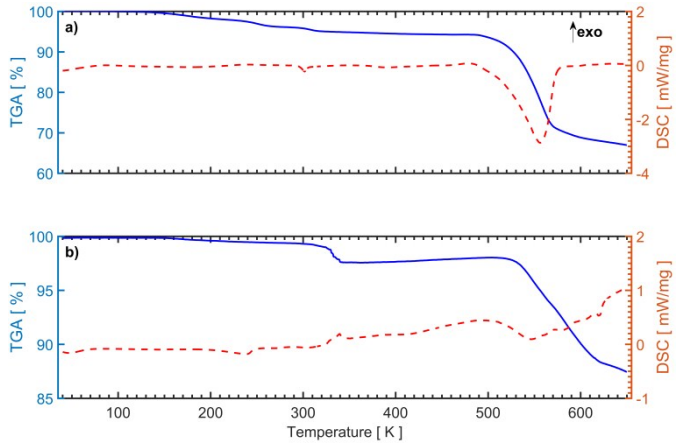


Figure S30. TGA/DSC of $M_3Mg(BH_4)_5$: a) M = Rb prepared using a solvent-mediated method of synthesis, b) M = Cs prepared via a mechanochemical approach, eq. (4), heating rate: 5 °C $min^{-1}$.

For the sample of $Rb_3Mg(BH_4)_5$ obtained in a solvent-mediated process a gradual mass loss starts above *ca.* 120 °C which is related to the emission of various organic impurities, resulting in a mass loss of *ca.* 4 wt%, Fig. S27. This process is rather well resolved from the endothermic release of hydrogen (*ca.* 1.2 wt%) occurring within the range of 290–350 °C. The integrated MS signal from the organic impurities is close to the integrated signal of hydrogen, which indicates a relatively high degree of contamination of investigated $Rb_3Mg(BH_4)_5$ sample (estimated purity of 83–96 wt% according to the yield of synthesis and TGA/MS data) in comparison to *e.g.* $Li[Zn_2(BH_4)_5]$, where the estimated purity >99 wt% has been achieved.[ix] At 480 °C a weakly exothermic process precedes the strongly endothermic event (*ca.* +320 kJ per mol of Mg) related to a substantial mass loss of >24 wt%. Volatile decomposition products are evolved till the end of the measurement (650 °C), resulting in the residual mass of 67%. Despite a huge mass loss the ion current corresponding to hydrogen emission is the only signal showing maximum in this range of temperature on the time-resolved MS plot. However, the M/Z signals from $H_2O$ (18, 17, 16) and $O_2$ (32), which are present in minor amounts in the carrier gas (Ar), significantly diminish their intensity, which implies that they might be consumed by Rb vapors which could form at such a high temperature.

$Cs_3Mg(BH_4)_5$ prepared mechanochemically, according to eq. (4), contains *ca.* 14.6 wt% LiCl. For this sample thermal decomposition is preceded by an endothermic event close to 235 °C which could be a sign of melting or a solid-state phase transition as it related only to a minor loss of mass (<0.4 wt%). Upon further heating an exothermic process is observed with the maximum at *ca.* 338 °C, which corresponds to *ca.* 1.7 wt% emission of hydrogen. The second significant mass drop occurs here above 510 °C and continues till the end of measurement (650 °C) resulting in residual mass of 87 wt%. As in Rb analogue, $H_2$ is released during this higly-endothermic process (the estimated enthalpy about +230 kJ per mol of Mg) with subsequent decrease of intensity of $H_2O$ and $O_2$ signals, which is most probably caused by a gradual emission of Cs vapors.


[i] P. Schouwink, M. B. Ley, T. R. Jensen, L. Smrčok and R. Černý, Dalton Trans., 2014, **43**, 7726.
[ii] J. Yang, J. Zheng, X. Zhang, Y. Li, R. Yang, Q. Feng and X.Li, Chem. Commun., 2010, **46**, 7530.
[iii] A. Talapatra, S. K. Bandyopathyay, P. Sen, P. Barat, S. Mukherjee and M. Mukherjee, Physica C, 2005, **419**, 141.
[iv] E. B. Lobkovskii, L. V. Titov, S. B. Psikha, M. Yu. Antipin, and Yu. T. Struchkov, Zh. Strukt. Khim. (Russ.) (J. Struct. Chem.) (1982) **23**, 172.
[v] V. D. Makhaev, A. P. Borisov, A. S. Antsyshkina, and G. G. Sadikov, Zh. Neorg. Khim. (Russ.) (Russ. J. Inorg. Chem.) (2004) **49**, 371.
[vi] P. Schouwink, V. D'Anna, M. B. Ley, L. M. Lawson Daku, B. Richter, T. R. Jensen, H. Hagemann and R. Černý, J. Phys. Chem. C, 2012, **116**, 10829.
[vii] V. D'Anna, A. Spyratou, M. Sharma, and H. Hagemann, Spectrochim. Acta A Mol. Biomol. Spectrosc., 2014, **128**, 902.
[viii] http://webbook.nist.gov/chemistry/
[ix] T. Jaroń, P. Orłowski, W. Wegner, K. J. Fijałkowski, P. J. Leszczyński and W. Grochala, Angew. Chem., Int. Ed. Engl., 2015, **54**, 1236.